Optical properties of calcium

P. O. Nilsson and G. Forssell
Department of Physics, Chalmers University of Technology, Fack, S-402 20 Gothenburg, Sweden

(Received 19 April 1977)

The optical constants of Ca have been determined from reflectance measurements in the range 2–11 eV. Good agreement with a calculation of the optical joint density of states is obtained. The origin of the absorption spectrum has been analyzed using plots of so-called optical surfaces. Studies of the dielectric function reveal two volume and two surface plasmons.

I. INTRODUCTION

Calcium precedes the 3*d* metals in the Periodic Table and is thus expected to have an unoccupied *d*-band complex just above the Fermi level. In agreement with this, recent band calculations show a *d*-band complex with its bottom close to the Fermi level and its top 6–7 eV higher. The position of the *d* band has important consequences for many properties of calcium. Of these, the most well known is the metal-semiconductor transition which occurs at high pressure.[1,2] This motivates research to establish the details of the band structure. Valuable information can be obtained by comparison between suitable spectroscopic data and the corresponding spectra calculated from the band structure. Measurements of soft x-ray absorption,[3] uv photoemission,[4] and appearance-potential spectroscopy[5] show correlations with some band calculations. Evaluation of these experiments has permitted the establishment of the approximate location and width of the *d*-band complex. Measurements of optical properties sometimes provide accurate determination of special features such as individual bands and are thus of complementary value. As the optical properties of calcium were not previously known we have found it worthwhile to determine these over a broad energy range and to calculate the corresponding functions from the band structure for comparison.

II. EXPERIMENTAL

A. Sample preparation

The specimens were prepared by evaporation from a tungsten basket on to a smooth quartz substrate. The calcium was in the form of shots of 99.5% purity. We know from earlier experiments on photoemission[4] from calcium that reproducible results can be obtained only after several successive evaporations. Because of this we performed outgassing of the source and pre-evaporations prior to the evaporation which produced the sample. We did not prepare films on top of each other for serious measurements because the surface seems to become rough. This produces erroneous results due to scattering, particularly in the uv range. The base pressure in the chamber was 2×10^{-10} Torr. During evaporation the pressure rose to 5×10^{-8} Torr, but, within 1 min of finishing evaporation, the pressure decreased to approximately 10^{-10} Torr again. The reflectance measurements were made *in situ*.

B. Reflectance measurements

Two different reflectometers were used to determine the optical constants of calcium. In one of them the near-normal-incidence (1.7°) reflectance was determined. The principle of the apparatus is shown in Fig. 1. The radiation from a one-meter normal incidence vacuum-ultraviolet grating monochromator (McPherson 225) passes a LiF window after which it is reflected in a toroidal mirror. The mirror can be rotated from the outside of the specimen chamber around an axis in the prolongation of the incident beam. By rotation of the mirror, the light beam hits the detector either directly or via the sample. The shape of the mirror has been chosen so that the width of the light spot on the detector is the same in the two positions. Under this condition the quotient of the two signals gives the reflectance of the sample. The detector is a photomultiplier placed

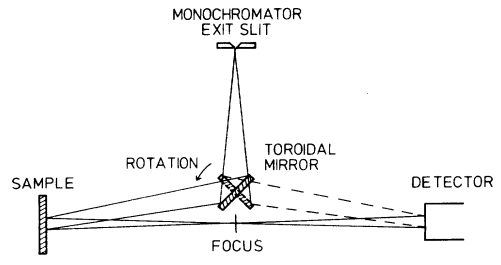

FIG. 1. Geometry of near-normal-incidence reflectometer.

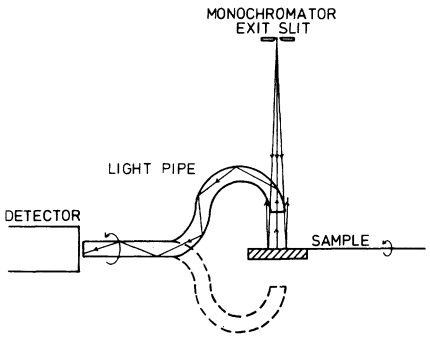

FIG. 2. Geometry of variable-incidence reflectometer.

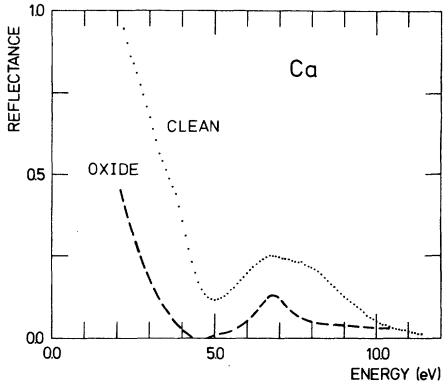

FIG. 3. Reflectance of clean and oxidized calcium.

outside the ultrahigh vacuum chamber. The light passes out of the chamber through a LiF window, then through a compartment filled with argon gas, and it finally hits a quartz plate coated with sodium salicylate in front of the photomultiplier tube. The uv light is in this way converted to light of longer wavelengths which can be detected.

As will become evident later, the near-normal measurements must be complemented with some extra information before the optical constants can be accurately computed. This can be achieved by using a reflectometer with variable incidence angle. The geometry of this reflectometer is shown in Fig. 2. The sample can be rotated to obtain various angles of incidence. The light pipe is then rotated to detect the reflected intensity. By removing the sample out of the light beam the intensity of the incident beam can be measured so that the data can be normalized to absolute reflectance. Although this reflectometer gives the optical constants directly, it was not convenient, for several reasons, to use it over the whole energy range. Firstly, it gives inaccurate data in some energy regions due to the particular values of the optical constants there. Secondly, the sample must frequently be removed from the light beam to check the stability of the source, a procedure which can introduce errors because of slight changes in alignment of the optical system.

The measurements of absolute reflectance is in general very difficult and can seldom be performed better than to an accuracy of about 0.01, a level which is estimated to be reached in the present work. The relative accuracy is, however, much better, and in the present case it is about 0.001. The critical factor for a good sample is the perfection of the optical system. As the detector has an area of varying sensitivity, beam inhomogeneities and beam displacements, etc. will give rise to incorrect absolute values. We have minimized these errors by accurate alignment, which was achieved by fine adjustments of the various components such as the sample holder, light pipe, etc. For details we refer to a more detailed report.[6]

III. RESULTS AND DISCUSSION

A. Experimental data

The reflectance of calcium in the energy region of 2.1 to 11.5 eV at normal incidence is shown in Fig. 3. The data has been confirmed through a second independent measurement. The two curves agree within 0.01 units. Annealing of the specimen at 160 °C for 3 h increased the reflectance only slightly in the region 2.5 to 3.5 eV as well as around 7 eV. The result of oxygen exposure of 1 Torr for 10 min can be seen in Fig. 3. A large drop in reflectance is observed. The minimum at 5.0 eV for clean calcium is shifted to 4.5 eV and corresponds to practically zero reflectance. The broad peak at around 7 eV is sharpened and occurs at 6.8 eV. The sample was found to be completely transparent to the eye.

As will become clear below we needed the optical constants for a few energies (in the present

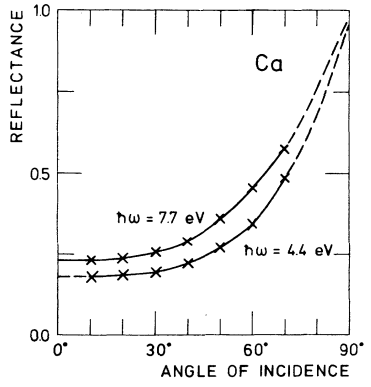

FIG. 4. Reflectance of calcium as a function of angle for 4.4- and 7.7-eV photon energy.

TABLE I. Values of refractive index $n+ik$ for Ca at two photon energies as obtained with the variable incidence reflectometer. The refectance R and phase shift θ are calculated from these data. R_{meas} is the directly measured reflectance with the near-normal-incidence reflectometer. p is the calculated polarization of the incident light.

$h\nu$	n	k	p	θ	R	R_{meas}
4.4	0.711	0.748	0.024	1.5274	0.1861	0.1985
7.7	0.541	0.671	0.030	1.7601	0.2372	0.2329

case we chose two energies) to be able to convert the reflectance curve to an absorption curve. This supplementary data was obtained by the use of the variable incidence reflectometer. The results of these measurements at 4.4 and 7.7 eV are given in Fig. 4.

B. Numerical treatment of the data

The reflectance of light with a polarization degree p and with an angle of incidence ϕ is a continuous function $R=R(n,k,p,\phi)$. If the reflectance for three angles ϕ_i is measured to R_i, $i=1,2,3$, respectively, we can find the complex refractive index $n+ik$ by solving the following equation system:

$$F(R_i,n,k,p,\phi_i)=0, \quad i=1,2,3\,.$$

We have worked out an iterative procedure to solve this problem. The 7 data points in Fig. 4 allow 35 equation systems to be solved, each of which ideally should give the same result. However, due to measuring errors, some combinations give a more reliable result than others. We have chosen to take the mean value only from those combinations which give a calculated reflectance at normal incidence, which is not far from the directly measured value at 10°.[6] A second criterion is that the polarization, p, should not deviate strongly from a mean value, which we found to be close to zero. The result of the analysis is shown in Table I.

The optical constants n and k were obtained over the whole energy range by dispersion analysis. For this purpose the reflectance data were smoothly extrapolated to $R=1.0$ for zero photon energy, $\omega=0$. The phase shift at an energy ω_0, caused by the reflectance up to the upper limit of the measured region, $\omega_u=11.5$ eV, was then calculated from

$$\theta'(\omega_0)=-\frac{\omega_0}{\pi}P\int_0^{\omega_u}\frac{\ln[R(\omega)/R(\omega_0)]}{\omega^2-\omega_0^2}\,d\omega\,. \qquad (1)$$

If the ln function is fitted to a second-order polynomial, the integral is analytically solvable and the pole is automatically avoided. The rest of the phase shift can be obtained from the expression[7]

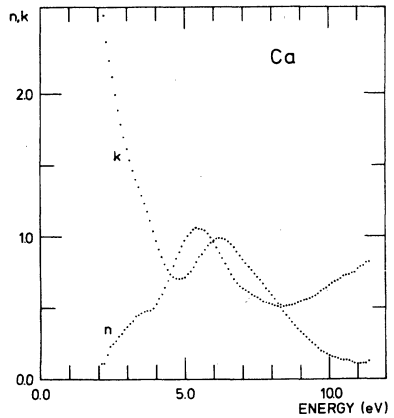

FIG. 5. Complex refractive index $n+ik$ for calcium obtained from the data in Figs. 3 and 4.

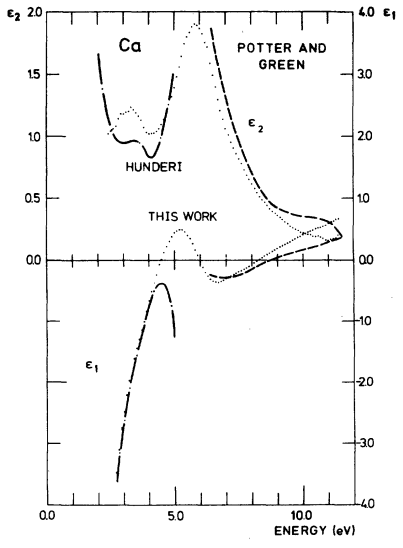

FIG. 6. Complex dielectric function $\epsilon_1+\epsilon_2$ for Ca obtained in this work compared to the results by Potter and Green (Ref. 8) and Hunderi (Ref. 9).

$$\Delta\theta(\omega_0) = -\frac{1}{2\pi}\ln\frac{R(\omega)}{R(\omega_0)}\ln\left|\frac{\omega_u-\omega_0}{\omega_u+\omega_0}\right| + \frac{\omega_u}{\pi}(\gamma_0+\gamma_2\omega_0^2). \quad (2)$$

The γ coefficients were determined by equating $\theta' + \Delta\theta$ to the phase shift at 4.4 and 7.5 eV as given in Table I. Finally n and k were calculated from R and θ through standard formulas. The result is shown in Fig. 5. A region of, at most, 1 eV at the low and high energy boundary may be somewhat distorted due to the extrapolation used.

In Fig. 6 the real and imaginary parts of the dielectric function $\tilde{\epsilon} = (n+ik)^2$ have been plotted. The curves are compared to data which have appeared in literature in the course of the present work.[8,9]

C. Interpretation

1. Absorption

Several band-structure calculations on Ca have appeared during the last few years.[4,10-14] In two cases the optical joint density of states (JDOS) were calculated. The result by Nilsson *et al.*[4] is shown in Fig. 7 (divided by ω) together with our experimental optical conductivity $\sigma = \omega nk/2\pi$. As is seen, there is an agreement in overall shape between the curves. They are further characterized by two peaks. The experimental peaks appear as mentioned at 3.7 and 6.0 eV, while the theoretical ones are found at 3.9 and 6.5 eV, respectively. The result by Lopez-Rios and Sommers[10] also contains two peaks, situated at 2.9 and 5.1 eV. The crystal potential was in principle constructed in the same way in both of the investigations, with the exchange parameter $\alpha = \frac{2}{3}$. We will in the following identify the two observed peaks with the peaks in the JDOS curve by Nilsson *et al.*,[4] thus assuming that the discrepancy is quantitative rather than qualitative.

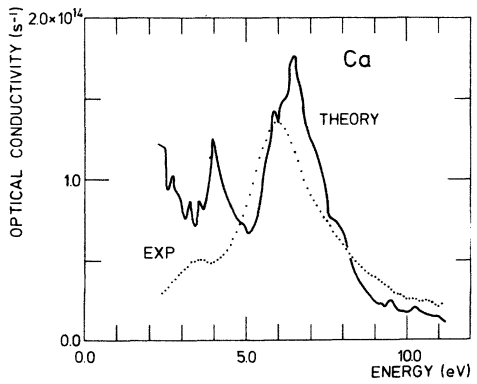

FIG. 7. Experimental optical conductivity of Ca compared to a calculation from the band structure in Fig. 8 with constant matrix elements.

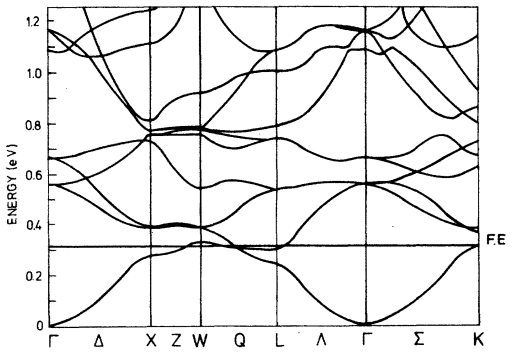

FIG. 8. Band structure of Ca in symmetry directions obtained by Nilsson *et al.* (Ref. 4).

The band structure is shown in Fig. 8. It is characterized by a nearly-free-electron-like band below the Fermi level and a $3d$-band complex at the Fermi level and extending about 6 eV upwards. It is evident from our earlier studies using uv photoemmision[4] and appearance potential spectroscopy[5] that this is a good starting approximation to the band structure.

A common scheme noted in the literature on analysis of optical data is to study the band structure in symmetry directions only. Such a procedure can sometimes give an approximate idea about the origin of the observed structure. However, for detailed, definite conclusions the complete band structure has to be used as will now be demonstrated.

In the first step of our analysis we resolve the total conductivity into partial contributions corresponding to transitions between band pairs. The result is shown in Fig. 9. From this figure we conclude that the experimental spectrum is a composite of transitions from band 1 to bands 4, 5, and 6. We shall show the analysis of the 3.7-eV peak here. In Fig. 10 a sequence of optical surfaces for the $1 \rightarrow 4$ transition is shown. We observe that the transitions start on a small area close to the hexagonal face. It develops rapidly and makes contact with the zone boundary. The maximum in $\sigma(\omega)$ occurs for 3.9 eV. Above this energy the surface leaves the boundary and moves towards the center of the zone, approaching a nearly-free-electron shape. The optical surface behaves *qualitatively* as in the case of so-called "parallel band absorption," which occurs in, for example, Al, and causes strong peaks in the optical conductivity. The specific feature of this kind of absorption is that at *threshold* the bands in a simple two-band

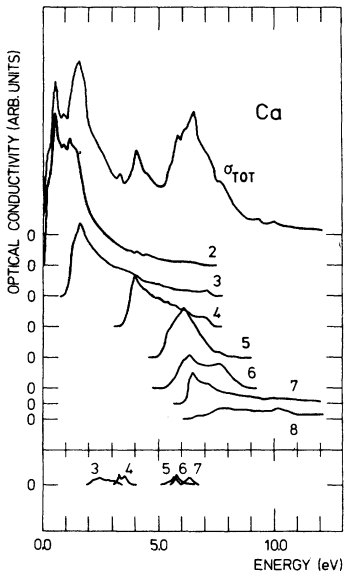

FIG. 9. Optical conductivity of Ca, σ_{tot}, calculated with constant matrix elements from the band structure in Fig. 8. The curves there below, labeled from 2 to 8, are the partial contributions to σ, corresponding to transitions from the lowest band, number 1, to higher bands. The curves at the bottom of the figure, labeled from 3 to 7, correspond to transitions from band number 2 to higher bands.

model are parallel not only in the two dimensions of the optical surface, but also in a third direction. This occurs because absorption starts at the Brillouin-zone boundary where the gradients of the bands in a two-band model are zero perpendicular to the boundary. It should be noted that above the threshold there is no qualitative difference between the so-called "normal" and "parallel-band" absorption.

Inspection of Fig. 10 shows a distortion from pure free-electron behavior: the absorption starts just inside the boundary and then makes contact with it gradually. This distortion is expected as the final bands are not very free-electron-like.

By examining the other items of structure in terms of optical surfaces, we find that the conventional way of interpretation, by using the band structure in symmetry directions only, can be misleading. Figure 10 demonstrates a fairly common situation, namely, that the structure is associated with the optical surfaces emerging at the Brillouin-zone boundary. As the bands here have a vanishing gradient in all three directions, a large volume in the k space (for a given energy resolution) contributes, giving rise to a maximum in the optical conductivity.

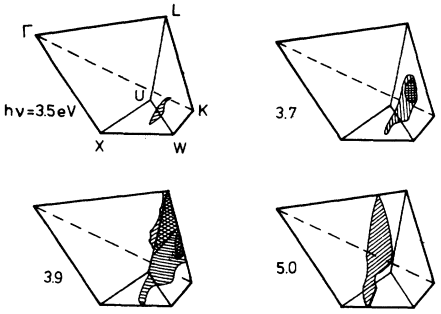

FIG. 10. Optical surfaces for the transition from the lowest band, number 1, to band number 4, for four photon energies.

2. *Plasmons*

In Fig. 11 we show the entities $\mathrm{Im}(1/\tilde{\epsilon})$ and $\mathrm{Im}(1/\tilde{\epsilon}+1)$ as calculated from our experimentally determined optical constants. The functions are proportional to the intensity of energy loss of fast electrons passing through the material. The losses are due to excitations of single electrons as in optical absorption, but also to volume and surface plasmons. Our data are compared with those of Potter and Green[8] obtained also from optical experiments. The results of characteristic energy-loss experiments by Kunz[15] are also shown. The energies of the various peaks in Fig. 11, as well as from some other experiments, are summarized in Table II.

The free-electron plasmon energy corresponding to the electron density of Ca is 8.0 eV. We obtain an energy of 8.8 eV for the volume plasmon in

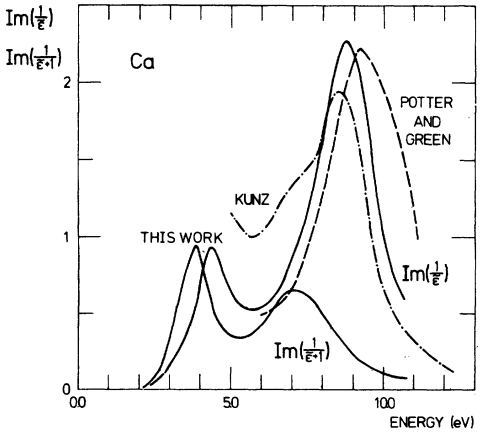

FIG. 11. Energy-loss functions calculated from our optical data compared with the corresponding ones by Potter and Green (Ref. 8) and with the characteristic loss data by Kunz (Ref. 15).

TABLE II. Experimental volume and surface plasmon energies for Ca as obtained by characteristic electron energy-loss experiments (upper part) and by optical experiments (lower part).

Authors	Volume plasmon (eV)		Surface plasmon (eV)	
Leder [a,b]	8.9	4.2		
Powell [c]	9.8	3.7		
Kunz [d]	8.7	4.1	6.8	1.8
Robins and Best [e]	8.8	3.4		
Potter and Green [f]	9.3		7.5	
Hunderi [g]		4.4		4.0
Present work	8.8	4.4	7.0	3.9

[a] Reference 16.
[b] Reference 17.
[c] Reference 18.
[d] Reference 15.
[e] Reference 19.
[f] Reference 8.
[g] Reference 9.

close agreement with, for example, the directly measured value of 8.7-eV by Kunz.[15] There is a small discrepancy to the value 9.3 eV by Potter and Green.[8] However, we prefer our value as it agrees with most of the characteristic loss experiments, where the resonance is directly measured. The value obtained from an optical experiment is calculated and often strongly dependent on the absolute magnitude of the optical constants. For the "surface plasmon" we obtain 7.0 eV, again close to the value of 6.8 eV by Kunz[8] and, with some larger deviation, to the value by Potter and Green.[15] The resonance is very strongly influenced by the interband transitions around 6 eV, which pushes the energy upwards. The free-electron value is 5.7 eV. In fact the ordinary condition for the existence of a surface plasmon, $\epsilon_1 = -1$, is not fulfilled. The resonance is strongly hybridized and is associated with a minimum in ϵ_1 *and* in ϵ_2 and it is thus a matter of taste what we call the resonance.

Calcium exhibits the rather unusual property of having two volume plasmons. At lower energies, we find at 4.4 eV the other volume loss. It occurs because the strong absorption peak around 6 eV causes ϵ_1 to make an oscillation so that it passes through zero at 4.5 eV, where ϵ_2 is still not too large, see Fig. 6. The situation is the same as for Ag, which exhibits a well-known example of a hybrid-type plasmon resonance, lowered to about half the free-electron value. Finally we find a surface-plasmon resonance at 3.9 eV. This can also be deduced from the optical constants by Hunderi.[9] From this data we find 4.0 eV. The value of 1.8 eV by Kunz[10] is surprising and we have no explanation for this discrepancy other than that a contamination (oxidation) of the sample could be the cause of the shift. The other resonances measured by Kunz are not expected to be as sensitive to such an effect.

D. Summary

The optical constants of calcium have been determined in the range 2–11 eV. The optical absorption has been found to be associated with interband transitions into the empty $3d$ band. The data verifies our earlier calculated band structure[4] which shows a $3d$ band extending from the Fermi level and about 6 eV up. The absorption spectrum has been analyzed in detail using plots of "optical surfaces" obtained from the band structure. These are locations in k space where the transitions take place for a given photon energy. It is found that peaks in the conductivity are typically associated with contact between the optical surface and the Brillouin-zone boundary, creating a large contributing k volume per photon energy interval. The analysis shows that an even better band structure would be obtained if the exchange-correlation contribution is somewhat increased above the present value $\alpha = \frac{2}{3}$, perhaps to 0.7.

Analysis of the complex dielectric function shows that two volume and two surface plasmons exist. The "ordinary" volume plasmon occurs in our data at 8.8 eV. The other plasma resonances are found at lower energies and are strongly influenced by interband transitions.

[1] R. A. Stager and H. G. Drickamer, Phys. Rev. 131, 2524 (1963).
[2] R. A. Ballinger and B. R. Allen, J. Phys. F 5, 1135 (1975).
[3] C. Sugiura, Jpn. J. Appl. Phys. 11, 598 (1972).
[4] P. O. Nilsson, G. Arbman, and D. E. Eastman, Solid State Commun. 12, 627 (1973).
[5] J. Kanski and P. O. Nilsson, Phys. Scr. 12, 103 (1975).
[6] G. Forssell, thesis (University of Gothenburg, 1976) (unpublished).
[7] P. O. Nilsson and L. Munkby, Phys. Kondens. Mater. 10, 290 (1969).
[8] M. R. Potter and G. W. Green, J. Phys. F 5, 1426 (1975).
[9] O. Hunderi, J. Phys. F 6, 1223 (1976).
[10] C. Lopez-Riod and C. B. Sommers, Phys. Rev. B 12, 2181 (1975).
[11] J. W. McCaffrey, J. R. Andersson, and D. A. Papaconstantopoulos, Phys. Rev. B 7, 674 (1973).
[12] S. Asano and J. Yamashita, J. Phys. Soc. Jpn. 35, 767 (1973).
[13] S. L. Altmann, R. C. Harford, and R. G. Blake, J.

Phys. F 2, 1062 (1972).
[14]M. Ross and K. Johnson, J. Phys. F 1, L13 (1971) and references therein.
[15]C. Kunz, Z. Phys. 196, 311 (1966).
[16]L. B. Leder, Phys. Rev. 103, 1721 (1956).
[17]L. B. Leder, Phys. Rev. 107, 1569 (1957).
[18]C. J. Powell, Proc. Phys. Soc. 76, 593 (1960).
[19]J. L. Robins and P. E. Best, Proc. Phys. Soc. 79, 110 (1962).